

Diffusion of tritons, deuterons, and protons in LiNbO_3 crystals

R. González and C. Ballesteros

Departamento de Física del Estado Sólido, Facultad de Ciencias Físicas, Universidad Complutense de Madrid, E-28040 Madrid, Spain

Y. Chen and M. M. Abraham

Solid State Division, Oak Ridge National Laboratory, P.O. Box 2008, Oak Ridge, Tennessee 37831-6032

(Received 8 August 1988)

Infrared absorption of OT^- , OD^- , and OH^- ions is used to monitor the presence of the three hydrogenic isotopes in LiNbO_3 single crystals. Tritium ions were produced by transmutation of the ${}^6_3\text{Li}$ nucleus via a $({}_0^1n, {}^4_2\text{He})$ reaction using thermal neutrons. OD^- ions were added to the crystal by subsequent heat treatments in D_2O vapor. There exist several configurations for each isotope, and each configuration is common to all three isotopes. Following isochronal heat treatments, the corresponding infrared bands for the three isotopes exhibit similar decay and growth behavior. Diffusion coefficients for all three hydrogenic species have been obtained. Between 900 and 975 K the diffusion coefficients were of the order of $10^{-7} \text{ cm}^2/\text{s}$.

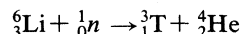
I. INTRODUCTION

In recent years, there has been increasing interest in understanding the fundamental properties of hydrogen impurities in oxide crystals. Hydrogen exists in most as-grown crystals as a ubiquitous impurity that profoundly influences the optical and electronic characteristics of oxide crystals, especially for device applications.¹⁻⁵ LiNbO_3 is an electro-optic crystal² that is widely used for linear, nonlinear, and laser-based electro-optic devices in information and image storage and coherent optical amplification.³⁻⁵ Laser optical damage, which limits the use of these devices even at moderate light power levels, may be reduced by the introduction of hydrogen in LiNbO_3 .^{6,7} Hydrogen can also prevent the out-diffusion of Li_2O during the heat treatments that are necessary in forming Ti-doped surface layers.⁸ In addition, protons have been identified as the mobile ions which neutralize the electronic space-charge field in the thermal fixing of volume holograms in iron-doped LiNbO_3 .⁹ These are examples of the property changes associated with the incorporation of hydrogen in LiNbO_3 .

In undoped LiNbO_3 the presence of hydrogen and deuterium in the form of OH^- and OD^- ions has been monitored by infrared-absorption measurements by several authors.^{6,10-13} The corresponding absorption bands occur at about 3480 and 2570 cm^{-1} , respectively. Their bandwidths are almost independent of whether the samples are measured at 295 or 77 K. For LiNbO_3 doped with Mg, a new narrower hydrogen band at about 3540 cm^{-1} has been observed.^{14,15} A band at about 3505 cm^{-1} has been reported for hydrogen close to the surface of LiNbO_3 crystals after proton exchange in benzoic acid.^{16,17}

In spite of the importance of tritium in advanced energy devices, very few data are available concerning the infrared characteristics and diffusion properties of tritium

in oxides.¹⁸⁻²⁰ The reason for this may be that experiments with tritium are hazardous and expensive. Recently tritium ions have been produced in LiNbO_3 crystals by transmutation of ${}^6\text{Li}$ ions.²¹ Tritium is produced by the following nuclear reaction:



with a production cross section²² of 910 b. The half-life of tritium is 12.36 yr. The natural abundance of the ${}^6_3\text{Li}$ isotope is 7.4%. The present study focuses on the infrared characterization of the absorption bands of OH^- and OT^- ions in LiNbO_3 single crystals after irradiation with thermal neutrons. The diffusion parameters of all three isotopic species (tritons, deuterons, and protons) have been determined. To our knowledge, there have been no published results on tritium diffusion parameters in the oxides.

II. EXPERIMENTAL PROCEDURES

The LiNbO_3 crystals used in the present study were cut perpendicular to the crystallographic z axis from boule no. 14N142, obtained from the Crystal Systems Division of the Union Carbide Corporation. Neutron irradiations were performed in a dry tube immersed in a D_2O tank (D3-1) of the Oak Ridge Bulk Shielding Reactor. The thermal neutron flux was $\sim 5 \times 10^{12} \text{ n cm}^{-2} \text{ s}^{-1}$, the fast neutron flux with energy exceeding 0.1 MeV was $\sim 0.6 \times 10^{11} \text{ n cm}^{-2} \text{ s}^{-1}$, and the γ flux was $0.7 \times 10^8 \text{ R/h}$. The duration of the irradiation was 40.8 h. The irradiation temperature was $\sim 310 \text{ K}$. Electron irradiations were carried out in vacuum using electrons from a 2.0-MeV van de Graaff accelerator (High-Voltage Engineering).

Infrared absorption measurements were performed with a Perkin-Elmer model 983 G. In all cases unpolarized light propagating along the crystallographic z axis

was used. Samples were heated in flowing air, oxygen, or D₂O vapor inside a quartz tube inserted in the horizontal, axial hole of a CHESA furnace.

III. MATHEMATICAL FORMALISM

The diffusion characteristics for a classical system with a low concentration of defects or impurities such that they do not interact with each other can be described by Ficks's second law; in an isotropic medium the rate of transfer of the diffusing species through a unit area of a section is proportional to the concentration gradient measured perpendicular to the section.²³ In one dimension, Ficks's second law can be written as

$$\frac{\partial C}{\partial t} = D \frac{\partial^2 C}{\partial x^2}, \quad (1)$$

where C is the concentration of the diffusing species, x is the coordinate, and D is the diffusion coefficient. For dilute systems, D can be considered independent of C .

General solutions of the diffusion equation can be obtained for a variety of initial and boundary conditions, provided the diffusion coefficient is constant.²³ Here we are dealing with the *out*- and *in*-diffusion of hydrogen isotopes.

(a) *Out*-diffusion. We are interested in diffusion out of a plane sheet of area S and thickness $2l$, through which the diffusing substance is initially uniformly distributed and the surfaces of which are kept at zero concentrations. Let C_0 be the initial concentration (at $t=0$) of the diffusing species in the sample and $C(x,t)$ be that at annealing time t . The diffusion equation,²³ is as follows:

$$C(x,t) = \frac{4C_0}{\pi} \sum_{n=0}^{\infty} \frac{1}{2n+1} \exp\left[-\frac{D_{\text{out}}(2n+1)^2\pi^2 t}{4l^2}\right] \times \sin\left[\frac{2n+1}{2l}\pi x\right]. \quad (2)$$

Equation (2) describes the diffusion of hydrogen isotopes to the surface of the sample as a function of crystal depth and diffusion time. However, in this study, the total concentration at time t , $C(t)$, of hydrogenic species in the sample was monitored by infrared optical absorption. Hence, Eq. (2) must be integrated over the crystal thickness before comparison with experiments can be made:

$$C(t) = \frac{1}{2l} \int_{-l}^l C(x,t) dx. \quad (3)$$

In writing Eq. (3), we neglected the diffusion through the edges of the sample and treated the problem as one dimensional. This is justified because the samples used in our experiment were thin ($l \ll S$).

Integration of Eq. (3) yields

$$C(t) = \frac{8C_0}{\pi^2} \sum_{n=0}^{\infty} \frac{1}{(2n+1)^2} \exp\left[-\frac{D_{\text{out}}(2n+1)^2\pi^2 t}{4l^2}\right]. \quad (4)$$

This equation has the correct extrema: At $t=0$,

$$C(t) = \frac{8C_0}{\pi^2} \sum_{n=0}^{\infty} \frac{1}{(2n+1)^2} = C_0.$$

At $t \rightarrow \infty$, $C(t) \rightarrow 0$.

$C(t)$ in Eq. (4) is proportional to the optical absorbance $A(t)$ of the OH⁻, OD⁻, or OT⁻ in the crystal. Thus out-diffusion coefficients can be calculated from the slope M of a semilogarithmic plot of the absorbance after anneals of time t , $A(t)$, against isothermal annealing time using the expression

$$D_{\text{out}} = \frac{4Ml^2}{\pi^2}. \quad (5)$$

(b) *In*-diffusion. The procedure for analyzing the in-diffusion data was described previously by González *et al.*²⁴ It requires knowledge of the initial absorbance of the diffusing species, A_0 , the absorbance after anneals of time t , and the absorbance at saturation (after long anneals), A_{∞} . The in-diffusion coefficient can be obtained from the formula

$$D_{\text{in}} = \left[\frac{l}{2}\right]^2 \frac{\pi m^2}{(A_{\infty} - A_0)^2}, \quad (6)$$

where m is the initial slope for a plot of absorbance versus \sqrt{t} .

IV. RESULTS AND DISCUSSION

A. OH⁻, OD⁻, and OT⁻ bands in LiNbO₃

As we mentioned in the Introduction, the as-grown crystals exhibited an OH⁻ vibration band at ~ 3480 cm⁻¹ with a full width at half maximum (FWHM) of ~ 30 cm⁻¹. The structure of the band is a consequence of the existence of two slightly inequivalent orientations of the OH⁻ bond in the plane perpendicular to the c axis.¹⁰ A previous study²¹ demonstrated that after irradiation with thermal neutrons, the band at 3480 cm⁻¹ was absent and two new bands at ~ 3500 and 3550 cm⁻¹ appeared in the OH⁻ region. Their FWHM's were ~ 40

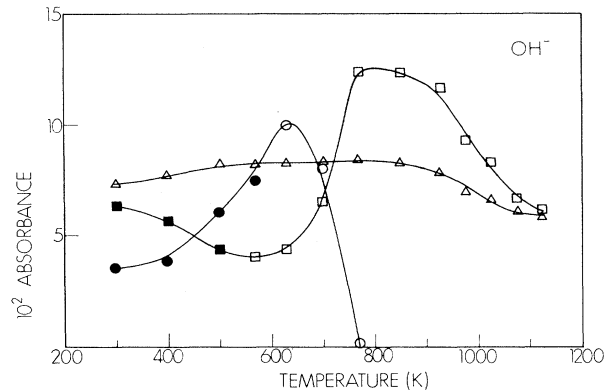


FIG. 1. Absorbance of OH⁻ bands vs isochronal annealing temperature for an n -irradiated crystal: ●, 3550 cm⁻¹; ○, 3545 cm⁻¹; ■, 3500 cm⁻¹; □, 3480 cm⁻¹. △ represents the absorbance at 3480 cm⁻¹ for an as-grown crystal.

and 20 cm^{-1} , respectively. In addition, two very weak bands at ~ 2180 and $\sim 2210\text{ cm}^{-1}$ were observed that have been associated with OT^- ions.

Figure 1 shows the behavior of the OH^- bands of an irradiated sample after isochronal anneals for 15-min intervals at increasing temperatures in air. The behavior of the OH^- band of an as-grown crystal is also shown for comparison. After the annealing at 570 K , the band at 3500 cm^{-1} disappeared and the band at 3480 cm^{-1} emerged. See Fig. 1 in Ref. 21. The intensity of the 3480 cm^{-1} band increased with anneals up to about 800 K , and then decreased at 1130 K to a value very close to that of the as-grown sample. Meanwhile, the band at $\sim 3550\text{ cm}^{-1}$ disappeared and a new band at 3545 cm^{-1} (FWHM of $\sim 15\text{ cm}^{-1}$) appeared. The intensity of the 3545 cm^{-1} reached a maximum at about 630 K . Thereafter, the intensity rapidly decreased and by 800 K was practically zero.

The behavior of the OT^- bands (Fig. 2) was similar to that described for the OH^- bands. The main difference was that the intensity of the 2180 - and 2211-cm^{-1} bands approached zero after annealing at 1130 K while the band at 3480 cm^{-1} is still apparent. This difference allows us to conclude that at these temperatures the H^+ out-diffusion is partially compensated by the H^+ out-diffusion from the water vapor in the air.

These observations indicate that during the neutron irradiation, protons were mobile and migrate to different OH^- configurations. Annealing at 800 K restored the initial configuration. The enhancement of proton diffusion by ionizing radiation has previously been observed in MgO single crystals.²⁵ During the neutron irradiation these crystals were exposed to a γ dose of $2.8 \times 10^9\text{ R}$. In order to determine whether ionizing radiation alone produces changes in the OH^- spectrum, an as-grown sample was irradiated in a ^{60}Co γ source up to a dose of $1 \times 10^9\text{ R}$ and another was electron irradiated with 1.5-MeV elec-

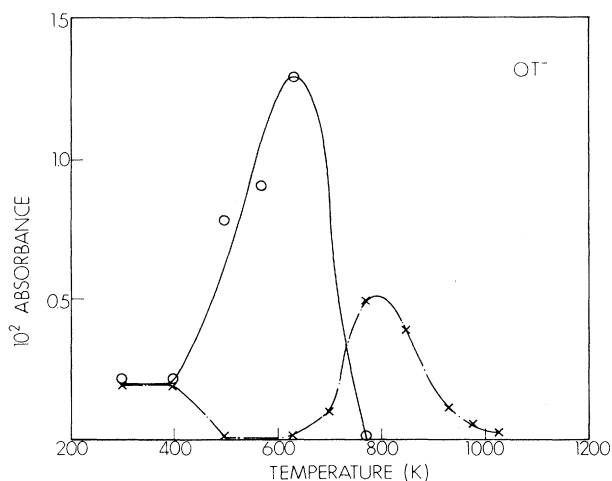


FIG. 2. Absorbance of OT^- bands vs isochronal annealing temperature for an n -irradiated crystal: \circ 2211 cm^{-1} ; \times , 2180 cm^{-1} .

trons up to a dose of $7 \times 10^{17}\text{ e cm}^{-2}$. No new bands in the OH^- spectrum were observed after either irradiation, indicating that ionizing radiation alone could not produce the changes observed in the neutron-irradiated crystals. Energetic neutrons accompanied the thermal neutrons, the former being 2 orders of magnitude lower in dose; the fast neutron dose was $8.8 \times 10^{15}\text{ n cm}^{-2}$. Assuming the defect production rate is similar to MgO ,²⁶⁻²⁸ the concentration of oxygen vacancies produced by the fast neutron is estimated to be $\sim 10^{17}\text{ cm}^{-3}$. The initially transparent crystals exhibited a slight brownish coloration after the neutron irradiation. Electron-irradiated crystals or reduced samples also exhibit a broad structure absorption band at about 500 nm .^{29,30}

The band at 3545 cm^{-1} has a FWHM which is half of that at 3480 cm^{-1} .²¹ The half-width of the 3500-cm^{-1} band is larger than that at 3480 cm^{-1} . A band at about 3535 cm^{-1} with a FWHM narrower than that at 3480 cm^{-1} has been observed in LiNbO_3 doped with high concentrations of magnesium.^{14,15} The presence of high concentrations of Mg drastically modifies vacancy concentration levels, since the excess positive charge of Mg^{2+} in a Li^+ site requires charge compensation. Following the previous discussion, these results indicate that the band at $3550\text{-}3545\text{ cm}^{-1}$ could be due to OH^- ions perturbed by oxygen vacancies. These vacancies would then anneal out during heat treatments, and at $\sim 800\text{ K}$ only the band

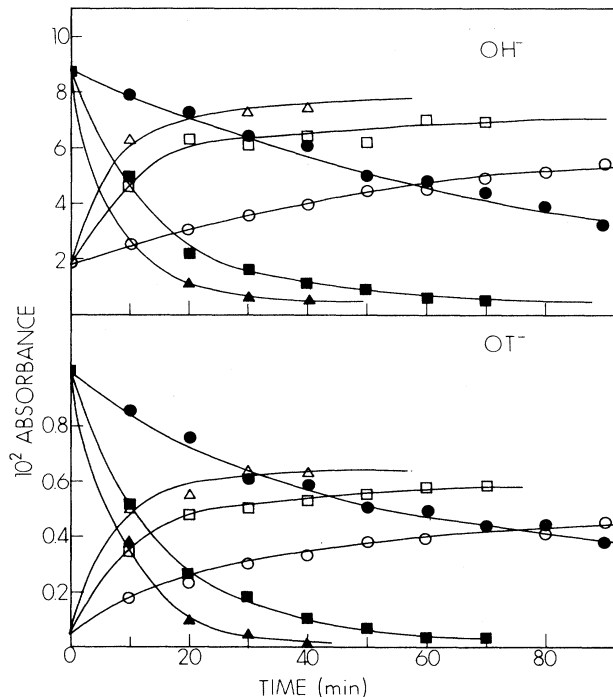


FIG. 3. Top: Absorbance of the OH^- bands at 3545 cm^{-1} (solid symbols) and 3480 cm^{-1} (open symbols) vs time for crystals isothermally annealed in flowing oxygen at 700 K (\bullet, \circ), 715 K (\blacksquare, \square), and 725 K ($\blacktriangle, \triangle$). Bottom: Absorbance of the OT^- bands at 2211 cm^{-1} (solid symbols) and 2180 cm^{-1} (open symbols) vs time for crystals isothermally annealed in flowing oxygen at 700 K (\bullet, \circ), 715 K (\blacksquare, \square), and 725 K ($\blacktriangle, \triangle$).

at 3480 cm^{-1} would be observed.

An examination of the decay kinetics of the 3545-cm^{-1} band and its tritium analogue at 2211 cm^{-1} has been carried out. Also, the growth kinetics of the 3480 cm^{-1} and its corresponding tritium band at 2180 cm^{-1} have been analyzed. Three neutron-irradiated samples were preannealed for 1 h at 600 K in flowing oxygen. After this treatment no band at 3500 cm^{-1} was observed, in agreement with the results presented in Fig. 1. The band at 3545 cm^{-1} (also the tritium analogue at 2211 cm^{-1}) was much more intense than the 3480-cm^{-1} band (2180 cm^{-1}). These crystals were subsequently isothermally heated for 10 min in flowing oxygen at 700, 715, and 725 K. Figure 3 illustrates the decay of the 3545- and 2211-cm^{-1} bands and the growth of the 3480- and 2180-cm^{-1} bands. These curves give the appearance of a mirror image of one another, indicating that most of the H^+ (T^+) occupying the configuration responsible for the 3545-cm^{-1} (2211-cm^{-1}) band moved into the new configuration resonating at 3480 cm^{-1} (2180 cm^{-1}). Assuming that the oscillator strength of the 3545- and 3480-cm^{-1} (or 2211- and 2180-cm^{-1}) bands is the same, the sum of the hydrogen concentration decreased with time. Furthermore, the decrease is more rapid at higher annealing temperatures. The decrease is attributed to out-diffusion of H^+ (T^+).

The activation energy E for the conversion of the 3545-cm^{-1} (2211-cm^{-1}) band into the 3480-cm^{-1} (2180-cm^{-1}) band may be obtained using the cross-cut method.³¹ In Fig. 4 the times for the three crystals to reach the same arbitrary absorbance value for the two hydrogen bands are plotted against the reciprocal of the annealing temperature, $1/T$. The slopes of these curves yield an activation energy of about $4.8 \pm 0.8\text{ eV}$ for the decay of the 3545-cm^{-1} band and $4.5 \pm 0.8\text{ eV}$ for the growth of the 3480-cm^{-1} band. Figure 5 is an Arrhenius plot for the two OT^- bands. The corresponding activation energies for the OT^- bands are 3.9 ± 1.0 and

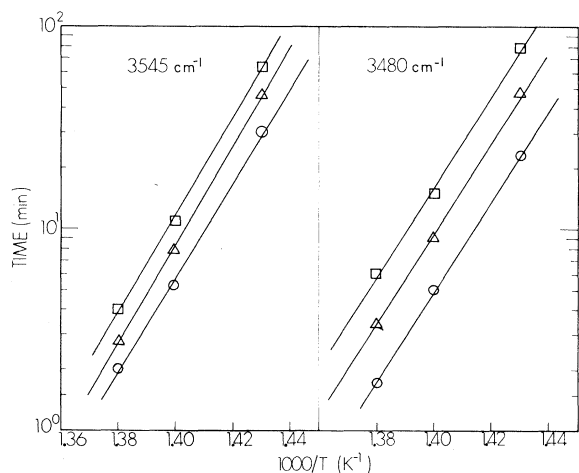


FIG. 4. Ln of the times for the three crystals (see Fig. 3, top) to reach the same arbitrary absorbance values at 3545 and 3480 cm^{-1} vs the reciprocal of the annealing temperature. Each curve was obtained for a different absorbance value.

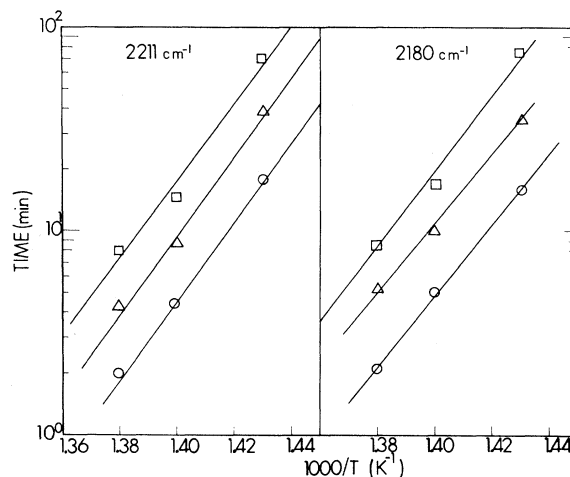


FIG. 5. Ln of the times for the three crystals (see Fig. 3, bottom) to reach the same arbitrary absorbance values at 2211 and 2180 cm^{-1} vs the reciprocal of the annealing temperature. Each curve was obtained for a different absorbance value.

$3.6 \pm 1.0\text{ eV}$, respectively. The tritium measurements are not as accurate as the hydrogen measurements because of the much lower tritium concentration. Also, the tritium bands occur near the band edge and are relatively more cumbersome to measure. These results demonstrate that the two isotopic bands exhibit similar behavior under heat treatment.

A band at 3505 cm^{-1} with a FWHM of $\sim 40\text{ cm}^{-1}$ has been previously observed^{16,17} in LiNbO_3 crystals after proton exchange in benzoic acid and has been attributed to hydrogen close to the surface since a light polish of the sample leads to a complete disappearance of this band. In order to check whether the band that we measured at

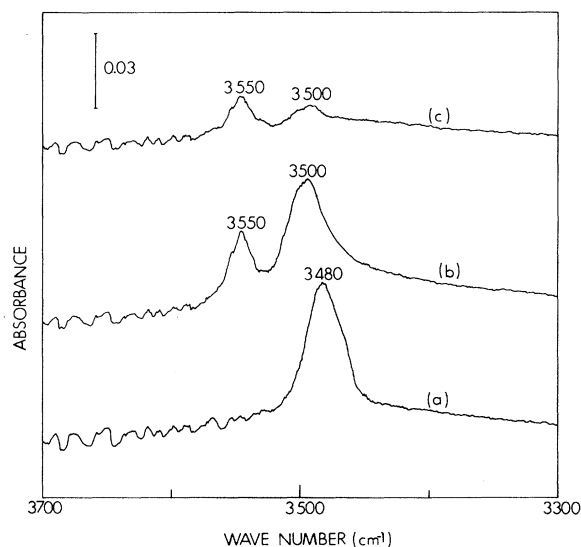


FIG. 6. Absorption spectra of (a) as-grown crystal, (b) after n irradiation, (c) after n irradiation and subsequent polishing of the crystal to remove $\sim 0.1\text{ mm}$ from each face. The initial thickness was 0.7 mm .

$\sim 3500 \text{ cm}^{-1}$ is also due to hydrogen concentrated at the surface, a neutron-irradiated sample was polished with diamond paste and approximately 0.1 mm of the material was removed from each face; the corresponding spectrum is shown in Fig. 6. The band at 3500 cm^{-1} decreased disproportionately faster than the band at 3550 cm^{-1} but it was not completely removed. However, when a virgin sample was heated in benzoic acid for 60 min at 473 K, a much lighter polishing completely removed the very intense band at 3500 cm^{-1} (Fig. 7). These results suggest that the 3500-cm^{-1} band observed in the neutron-irradiated sample is the same as that observed after heating in benzoic acid; furthermore, the H^+ responsible for the appearance of the 3500-cm^{-1} band in neutron-irradiated crystals was not completely localized at the surface region. In virgin samples annealed in benzoic acid with deuterium substituting for the hydrogen, a depth profile of deuterium concentration has shown that most of the deuterium is concentrated in a layer $1 \mu\text{m}$ thick.³² The high concentration of hydrogen or deuterium in the exchanged layer indicates that not all the H^+ or D^+ present substitute directly for Li atoms in the host lattice but that appreciable amounts of H^+ or D^+ likely occupy other sites, possibly including interstitial positions. The coincidence in peak position and FWHM of the 3500-cm^{-1} band in neutron-irradiated crystals with those of the band observed in samples heated in benzoic acid suggests that the band could be associated with OH^- vibrations for those hydrogen displaced during the irradiation into other sites. These protons would subsequently migrate to substitutional positions during the sample annealings at 400 and 573 K; consequently the intensity of the 3500-cm^{-1} band decreased and that of the bands at 3545 and 3480 cm^{-1} increased (Fig. 1).

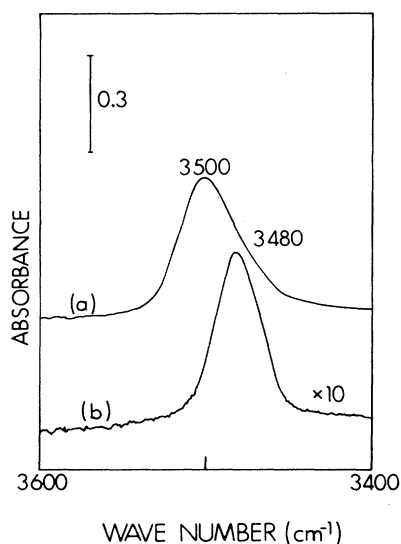


FIG. 7. Absorption spectra of (a) as-grown crystal after proton exchange for 60 min at 473 K in benzoic acid and (b) after a very slight polishing of the two faces.

B. Diffusion measurements

Proton and deuteron diffusion measurements in LiNbO_3 have generally been made using molten benzoic acid as the hydrogen source or benzoic acid with deuterium substituted for the acidic hydrogen as the deuterium source.³²⁻³⁴ Bulk diffusion of D^+ from D_2O vapor has also been studied.¹¹ Up to now, tritium diffusion measurements have not been reported either in LiNbO_3 or in other oxides. In this section, we will show our results both on the out-diffusion and in-diffusion characteristics of all three isotopic species (tritons, deuterons, and protons).

(a) Out-diffusion. Four neutron-irradiated samples were preannealed at 800 K for 1 h in flowing oxygen. After this treatment, only the bands at 3480 and 2180 cm^{-1} were observed. Three of these samples were used to determine the diffusion coefficients and activation energies for H^+ and T^+ out-diffusion in flowing oxygen at three different temperatures. The fourth one was used for experiments in D_2O vapor.

Figure 8 shows the decrease in the OH^- and OT^- absorbance bands versus time for the three crystals with the same thickness ($\sim 1 \text{ mm}$) and initial hydrogen and tritium concentration. These crystals were isothermally annealed in flowing oxygen at 900, 930, and 960 K. Using the cross-cut method³¹ on these curves, the resulting activa-

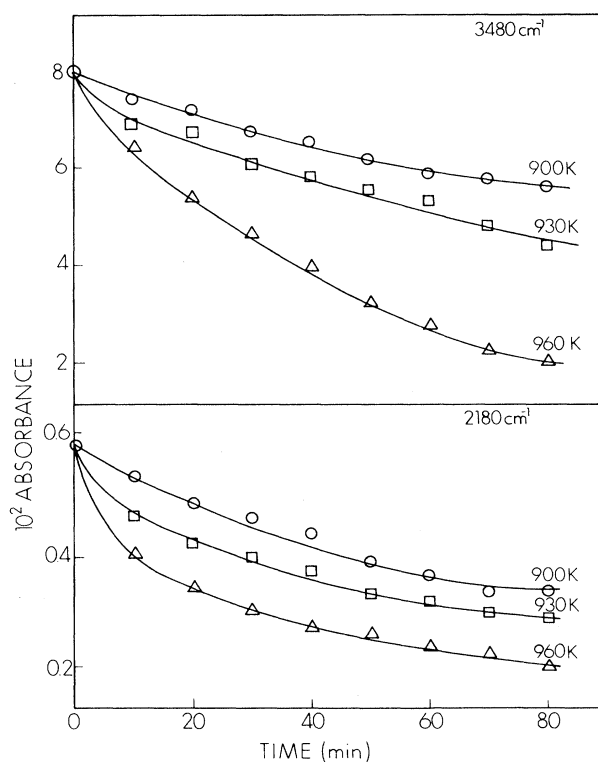


FIG. 8. Absorbance of the OH^- band at 3480 cm^{-1} (top) and of the OT^- band at 2180 cm^{-1} (bottom) against annealing time for three samples annealed in flowing oxygen at 900 K (\circ), 930 K (\square), and 960 K (\triangle), respectively. The samples were previously annealed in flowing oxygen for 1 h at 773 K.

TABLE I. Diffusion coefficients of hydrogen isotopes in LiNbO_3 .

T (K)	Out-diffusion coefficients ($10^{-8}\text{cm}^2/\text{s}$)		
	H^+	T^+	D^+
900 ^a	8±3	12±6	
930 ^a	12±5	13±6	
960 ^a	29±12	24±12	37±15 ^c
975 ^b	47±19	36±18	

^aDiffusion coefficients measured with the samples immersed in flowing oxygen.

^bSample preannealed in D_2O vapor.

^cDiffusion coefficients measured with the sample immersed in D_2O vapor.

tion energies for H^+ and T^+ out-diffusion were 1.9 ± 0.4 and 1.8 ± 0.4 eV. A semilogarithmic plot of the OH^- absorbances versus isothermal annealing time for the three temperatures yields, using Eq. (5), the diffusion coefficients for hydrogen: $D_{\text{out}}^{\text{H}}(900\text{ K})=(8\pm 3)\times 10^{-8}\text{cm}^2/\text{s}$, $D_{\text{out}}^{\text{H}}(930\text{ K})=(12\pm 5)\times 10^{-8}\text{cm}^2/\text{s}$, and $D_{\text{out}}^{\text{H}}(960\text{ K})=(29\pm 12)\times 10^{-8}\text{cm}^2/\text{s}$. For tritium, the diffusion coefficients are $D_{\text{out}}^{\text{T}}(900\text{ K})=(12\pm 6)\times 10^{-8}\text{cm}^2/\text{s}$, $D_{\text{out}}^{\text{T}}(930\text{ K})=(13\pm 6)\times 10^{-8}\text{cm}^2/\text{s}$, and $D_{\text{out}}^{\text{T}}(960\text{ K})=(24\pm 12)\times 10^{-8}\text{cm}^2/\text{s}$. We conclude that there is no significant difference between hydrogen and tritium out-diffusion from the crystals.

Out-diffusion of D^+ in flowing oxygen was performed using another sample. Initially the sample was heated in

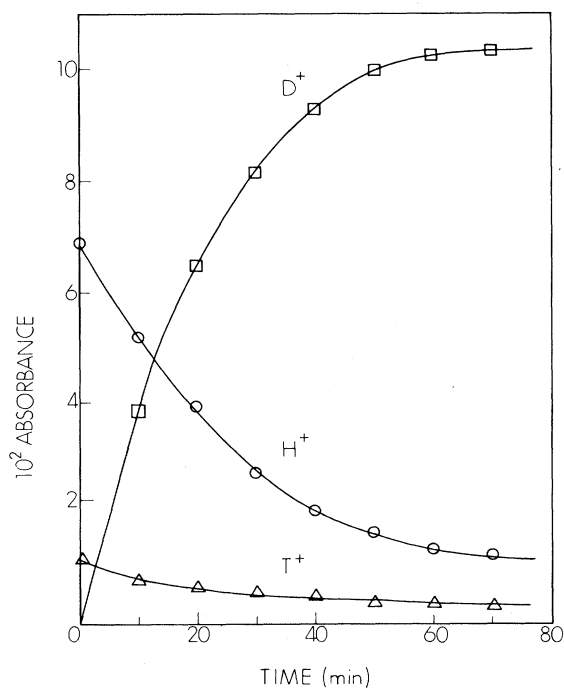


FIG. 9. Absorbance of OH^- , OD^- , and OT^- ions vs time for a crystal isothermally annealed in D_2O vapor at 975 K. The sample was previously annealed in flowing oxygen for 1 h at 773 K.

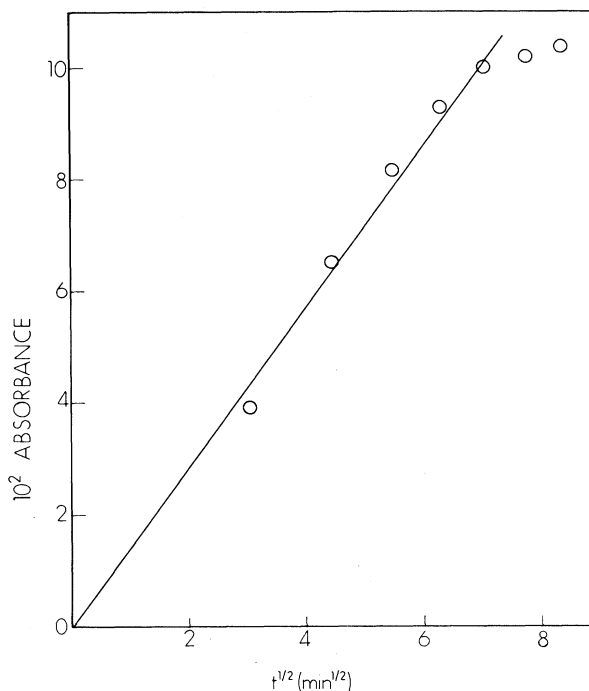


FIG. 10. Absorbance of OD^- ions at 2560 cm^{-1} vs \sqrt{t} for the sample in Fig. 9.

flowing D_2O vapor at 975 K until it was saturated with deuterons (see following paragraph). The diffusion coefficient for D^+ out-diffusion at 960 K was measured and the resulting value was $(37\pm 15)\times 10^{-8}\text{cm}^2/\text{s}$, which also agrees with those calculated for H^+ and T^+ out-diffusion at the same temperature. These results are summarized in Table I.

(b) In-diffusion. Although the out-diffusion results agree with those previously found for D^+ in-diffusion from D_2O vapor,¹¹ we performed an experiment that involves the exchange of D^+ with existing H^+ and T^+ ions. One sample (with the same thickness and initial hydrogen and tritium concentration of those plotted in Fig. 8) was isothermally annealed in D_2O vapor at 975 K. The absorbances at 3480, 2560, and 2180 cm^{-1} were measured after each anneal. Figure 9 provides clear evidence that the OD^- concentrations increased at the expense of the OH^- and OT^- concentrations. When the OD^- concentration approached saturation, the loss of the OH^- and OT^- slowed down. Prolonged annealing of this sample in D_2O vapor at 975 K yielded a saturation value (not shown in Fig. 9) of 0.12 for the absorbance of the OD^- band. This value corresponds to a higher concentration than the initial concentration of H^+ and T^+ .

Figure 10 plots the OD^- absorbance versus \sqrt{t} for the sample annealed in D_2O at 975 K. The diffusion coefficient for deuterium in-diffusion was calculated from the slope and the absorbance at saturation using Eq. (6). The resulting value was $D_{\text{in}}^{\text{D}}(975\text{ K})=(45\pm 18)\times 10^{-8}\text{cm}^2/\text{s}$. In addition we used this opportunity to obtain another data point for both hydrogen and tritium

out-diffusion at 975 K. A semilogarithmic plot of the OH^- and OT^- absorbances against annealing time yields the following diffusion coefficients for the H^+ and T^+ out-diffusion: $D_{\text{out}}^{\text{H}}(975 \text{ K}) = (47 \pm 19) \times 10^{-8} \text{ cm}^2/\text{s}$ and $D_{\text{out}}^{\text{T}}(975 \text{ K}) = (36 \pm 18) \times 10^{-8} \text{ cm}^2/\text{s}$.

V. SUMMARY AND CONCLUSIONS

LiNbO_3 crystals generally contain hydrogen and our crystals were no exception. Tritium and deuterium have been added to the crystals, the former by a transmutation of the ${}^6_3\text{Li}$ nucleus via a (${}^1_0n, {}^4_2\text{He}$) reaction using thermal neutrons, and the latter by diffusion in D_2O vapor. There exist several OH^- configurations, represented by different absorption peaks in the OH^- vibrational region of 3500 cm^{-1} . Corresponding OD^- and OT^- configurations were also observed in the vicinity of ~ 2500 and 2100 cm^{-1} , respectively. In general, each configuration for all three isotopes responds to thermal treatment in a similar manner; that is, the corresponding absorption bands decay or grow in parallel fashion.

After irradiation with neutrons, the OH^- absorption band at 3480 cm^{-1} vanished and new bands at 3500 and 3550 cm^{-1} emerged. The change in the OH^- spectrum is attributed to the combined effects of energetic neutrons ($> 1 \text{ MeV}$) and the attending gamma rays. Annealing at 800 K restored the original 3480-cm^{-1} band. The analogue OT^- bands exhibit similar behavior.

The activation energy associated with the thermal conversion of the 3545 into the 3480 cm^{-1} band, and the OT^- analogue 2211 into the 2180-cm^{-1} band, was determined to be between 3 and 5 eV .

The broad absorption band observed at 3500 cm^{-1} in the neutron-irradiated crystal appeared to be concentrated near the surface region. The concentration gradient was smaller than in a virgin sample heated in benzoic acid. It is suggested that not all the hydrogenic species substitute for Li^+ , but that other sites, including interstitials, are likely.

Diffusion coefficients based on out-diffusion of protons and tritons have been measured. Between 900 and 975

K , the diffusion coefficients are of the order of $10^{-7} \text{ cm}^2/\text{s}$. Within experimental accuracy, the values for H^+ and T^+ were similar. The activation energy for both species was $1.8 \pm 0.4 \text{ eV}$.

There exist several configurations for each of the three isotopes, corresponding to OH^- , OD^- , and OT^- ions within the infrared regions of ~ 3500 , 2500 , and 2100 cm^{-1} , respectively. The isotopic analogues for each configuration grow and decay with temperature in similar fashion, indicating that the different configurations are replicated for each isotope.

The diffusion properties of the hydrogenic isotopes in a given host are governed by three characteristics: (1) the charge, or valence, (2) the ionic size, and (3) the mass. In principle, some difference in the diffusion coefficient for the three isotopes can be expected. For all practical purposes, the charge and the ionic radii are the same for the three isotopes. However, the mass is different for hydrogen, deuterium, and tritium. Our results showed that if there is a difference in the diffusion characteristics for the three isotopes in LiNbO_3 , it is below our level of detectability. We conclude that the charge and/or the ionic size is much more important than the mass in affecting the diffusion behavior for hydrogen in LiNbO_3 , in agreement with previous findings in MgO , an oxide with a very different crystalline structure.²⁴

ACKNOWLEDGMENTS

The authors thank Dr. E. Hodgson and the staff of CIEMAT for the Van de Graaff electron irradiations. Helpful discussions with M. Gómez are gratefully acknowledged. This research was sponsored by the Comisión Asesora de Investigación Científica y Técnica of Spain, by the U.S. Defense Advanced Research Projects Agency under Interagency Agreement No. 40-1611-85 with the U.S. Department of Energy, and by the Materials Science Division, Office of Basic Energy Sciences, U.S. Department of Energy, under Contract No. DE-AC05-84OR21400 with Martin Marietta Energy Systems, Inc.

¹Y. Chen and R. González, *Opt. Lett.* **10**, 276 (1985).

²P. Gunter, *Phys. Rep.* **93**, 119 (1982).

³A. Räuber, in *Current Topics in Materials Science*, edited by E. Kaldis (North-Holland, Amsterdam, 1978), Vol. 1, p. 481.

⁴I. P. Kaminow, *An Introduction to Electro-optics Devices* (Academic, New York, 1974).

⁵G. Weber, S. Kapphann, and M. Wöhlecke, *Phys. Rev. B* **34**, 8406 (1986).

⁶R. G. Smith, D. B. Fraser, R. T. Denton, and T. C. Rich, *J. Appl. Phys.* **39**, 4600 (1968).

⁷J. L. Jackel, D. H. Olsen, and A. M. Glass, *J. Appl. Phys.* **52**, 4855 (1981).

⁸J. L. Jackel, V. Ramaswamy, and S. P. Lyman, *Appl. Phys. Lett.* **38**, 509 (1981).

⁹H. Vormann, G. Weber, S. Kapphann, and E. Krätzig, *Solid State Commun.* **40**, 543 (1981).

¹⁰J. R. Herrington, B. Dischler, A. Räuber, and J. Schneider, *Solid State Commun.* **12**, 351 (1973).

¹¹R. González, Y. Chen, K. L. Tsang, and G. P. Summers, *Appl. Phys. Lett.* **41**, 739 (1982).

¹²L. Kovács, V. Szalay, and R. Capelletti, *Solid State Commun.* **52**, 1029 (1984).

¹³A. Föster, S. Kapphann, and M. Wöhlecke, *Phys. Status Solidi B* **143**, 755 (1987).

¹⁴D. A. Bryan, R. Gerson, and H. E. Tomaschke, *Appl. Phys. Lett.* **44**, 847 (1984).

¹⁵D. A. Bryan, R. R. Rice, R. Gerson, H. E. Tomaschke, K. L. Sweeney, and L. E. Halliburton, *Opt. Eng.* **24**, 138 (1985).

¹⁶J. L. Jackel and C. E. Rice, *Ferroelectrics* **38**, 801 (1981).

¹⁷C. Canali, A. Carnera, G. Della Mea, P. Mazzoldi, S. M. Al Shakri, A. C. G. Nutt, and R. M. De la Rue, *J. Appl. Phys.* **59**, 2643 (1986).

¹⁸J. B. Bates and R. A. Perkins, *Phys. Rev. B* **16**, 3713 (1977).

¹⁹J. V. Cathcart, R. A. Perkins, J. B. Bates, and L. C. Manley, *J. Appl. Phys.* **50**, 4110 (1977).

²⁰H. Engstrom, J. B. Bates, and L. A. Boatner, *J. Chem. Phys.*

- 73, 1073 (1980).
- ²¹R. González, Y. Chen, and M. M. Abraham, *Phys. Rev. B* **37**, 6433 (1988).
- ²²A. Tollestrup, W. A. Fowler, and C. C. Lauritsen, *Phys. Rev. B* **78**, 372 (1950).
- ²³J. Crank, *The Mathematics of Diffusion* (Clarendon, Oxford, 1956).
- ²⁴R. González, Y. Chen, and K. L. Tsang, *Phys. Rev. B* **26**, 4637 (1982).
- ²⁵Y. Chen, M. M. Abraham, and H. T. Tohver, *Phys. Rev. Lett.* **37**, 1757 (1976).
- ²⁶W. A. Sibley and Y. Chen, *Phys. Rev.* **160**, 712 (1967).
- ²⁷Y. Chen, R. T. Williams, and W. A. Sibley, *Phys. Rev.* **182**, 960 (1969).
- ²⁸Y. Chen, D. L. Trueblood, O. E. Schow, and H. T. Tohver, *J. Phys. C* **3**, 2501 (1970).
- ²⁹E. R. Hodgson and F. Agulló-López, *Solid State Commun.* **64**, 965 (1987).
- ³⁰R. Pareja, R. González, and M. A. Pedrosa, *Phys. Status Solidi* **84**, 179 (1984).
- ³¹A. C. Demask and G. J. Dienes, *Point Defects in Metals* (Gordon and Breach, New York, 1963).
- ³²C. E. Rice, J. L. Jackel, and W. L. Brown, *J. Appl. Phys.* **57**, 4437 (1985).
- ³³C. M. Wassen, S. Forouhar, W. S. C. Chang, and S. K. Yao, *Appl. Phys. Lett.* **43**, 424 (1983).
- ³⁴J. L. Jackel, C. E. Rice, and J. J. Veselka, *Appl. Phys. Lett.* **41**, 607 (1982).